Supplementary material - Degree-of-linear-polarization-based Color Constancy

Taishi Ono Yuhi Kondo Legong Sun Teppei Kurita
Yusuke Moriuchi
Sony Group Corporation, Tokyo, Japan
{Taishi.Ono,Yuhi.Kondo,Legong.Sun,Teppei.Kurita,Yusuke.Moriuchi}@sony.com

This supplementary material is outlined as follows. References to the main paper (sections, equations, and figures) are highlighted in blue.

- Section 1 shows the description of the equation for chromatic pixels (Eq. 7).
- Section 2 is about how to handle the inherent ambiguity of the angle of linear polarization (AoLP) described in Sec. 3.5.
- Section 3 describes the detail of our evaluation data.
- Section 4 explains the settings we used for the existing methods.
- Section 5 describes the effect of different patch sizes for multi-illumination scenes shown in Sec. 5.
- Section 6 is the flow chart of our illumination estimation.

1. Details of equation for chromatic pixels

As described in Sec. 3.4, we assume a white-balanced color of a pixel becomes the opposite against its degree of linear polarization (DoLP) color. However, DoLP depends on the specular and diffuse Mueller matrices (M_s, M_d) as well as the specular and diffuse reflectances $(r_s, r_d(\lambda))$, as shown in Eq. 3. As a result, directly comparing the white-balanced color $\boldsymbol{i_{WB}} = (k_R i_\mathrm{R}, i_\mathrm{G}, k_B i_\mathrm{B})$ and DoLP (d_R, d_G, d_B) does not provide accurate results. Therefore, to disregard the domain difference between the white-balanced color and DoLP, they are subtracted by their averages and normalized by their l_2 norms, described in Eq. 7.

As shown in Fig. 3, this formulation estimates illumination colors (k_R, k_B) when observing two or more pixels. However, the formulation still includes several problems to be solved. Firstly, we assume the specular and diffuse polarization have different AoLPs, but the differences depend on the light and view directions. Therefore, when the differences are very small, the reliability of Eq. 7 could decrease. Considering the conventional polarization models have assumed that the AoLP differences are always 90 degrees [12], it is reasonable to assume that some differences always exist. Secondly, when scenes only include a few diffuse reflectances r_d, the obtained simultaneous equations become unstable. We would like to establish a more accurate and stable formulation for the chromatic pixels in the future.

2. Ambiguity of AoLP

In our calculation, AoLP is determined between 0° and 180°. When we compute w_{ach}^{aolp}, we define x and y in Eq. 9 as follows:

$$x = \min\left\{\left|AoLP_\mathrm{R} - AoLP_\mathrm{G}\right|, 180^\circ - \left|AoLP_\mathrm{R} - AoLP_\mathrm{G}\right|\right\} \tag{1}$$

$$y = \min\left\{\left|AoLP_\mathrm{B} - AoLP_\mathrm{G}\right|, 180^\circ - \left|AoLP_\mathrm{B} - AoLP_\mathrm{G}\right|\right\}. \tag{2}$$

Note that this kind of problem in AoLP is often referred to as an ambiguity problem in shape-from-polarization methods [2,6].

3. Evaluation data

3.1. Position of color chart

The evaluation data included a few multi-illumination scenes. In these scenes, firstly, we located a color chart in several positions and acquired corresponding white-balanced images. Secondly, we manually selected images that were the most suitable for human preferences. For instance, Fig. 1a and Fig. 1b represent the white-balanced images corrected by a color chart located on shadow and sunlit areas, respectively. Given that this scene was captured in the daytime, Fig. 1b is preferable to our perception. So we chose Fig. 1b as the ground truth. Note that we applied this procedure only for a few scenes in the data, and the difference between Fig. 1a and Fig. 1b was the most significant in those multi-illumination scenes. When we excluded these multi-illumination scenes and the blue-sky ones, the mean angular error of C4 [13] was 3.38, and ours was 3.24.

Additionally, we paid close attention to that a pair of images with and without the color chart shares the same illuminations. Note that the evaluation results were almost the same when we used the images including a color chart as our target images.

(a) White-balanced image 1. (b) White-balanced image 2.

Figure 1. For multi-illumination scenes, a color chart was located on several places. Firstly we acquire the images corresponding to each color chart, and then chose one result that were the most suitable for human preferences.

3.2. Acquire raw-RGB from capturing

For both cameras, we subtracted the dark current using a built-in function of the cameras. For the polarization camera FLIR BFS-U3-51S5PC-C, we replaced defected pixels with the average of the surrounding pixels of the same polarizer angles. For the polarization-demosaicking method of the polarization sensor, we used a method that considers frequency of pixel values by using the pixels located near the target pixel [7].

3.3. Personal information

All human faces included in our evaluation data were collected from those who approved the data usage. For license plates of cars, we filled the pixels with zero. When estimating illuminations, we input the filled pixels as they are. Note that only one image included the license plate, and the area was small, shown in Fig. 2.

Figure 2. License plates were filled with zero.

4. Settings for existing methods

For White-patch [8], Gray-world [4], and Chen *et al*. [5], we used parameters between 0 to 5, which determines the percentile of usable pixel intensity, and then chose the best results. For Gray-edge [11], we used the first derivative of images, which is often referred to as 1st-order Gray-edge. For FFCC [3], we estimated the illumination colors using all seven models provided by the authors and chose the best results. For FC4 [9], we used an implementation available from Rizzo [9]. For C4 [13], we applied the SqueezeNet backbone and used the average values of three estimations. Additionally, we set the dark current in the code as zero because it is already subtracted in our evaluation data. For C5 [1], it is necessary to input several images captured by the same cameras. Therefore, we separated our evaluation data into two groups according to the used camera and input seven images, which was the default number provided by the authors. Furthermore, we averaged the results of ten estimations for C5. For the method disregarding the diffuse polarization, we simply applied Fischer et al. [10] to each pixel and averaged them. Note that we excluded edges using w_{ch}^{aolp} with the same parameter when averaging the results. We did not include this result to our main paper because Fischer et al. [10] has several unknown parameters and we could not assure the fair comparison.

5. Effect of patch sizes for multi-illumination scenes

As described in Sec. 3.3, we can estimate the illumination color from only one pixel for achromatic pixels. Furthermore, theoretically, we can reconstruct the illumination color from at least two pixels for chromatic pixels, as shown in Sec. 3.4.

However, it is less likely to contain achromatic pixels when we use smaller patches. Additionally, the variation of diffuse reflectances included in the patches becomes smaller; thus, the simultaneous equations obtained by Eq. 8 become more unstable. Therefore, in the experiments shown in Sec. 5, we manually tried a few sizes of patches and subjectively selected the most natural results. We would like to investigate how to select the patch sizes automatically in the future.

6. Flow chart of estimating illuminations

Figure 3 is a flow chart describing the process from demosaicking to the final result $\hat{\boldsymbol{l}}$. $m(u,v)$, $n(u,v)$, and $o(u,v)$ denote $(d_{\mathrm{B}}-d_{\mathrm{G}})i_{\mathrm{R}}$, $(d_{\mathrm{G}}-d_{\mathrm{R}})i_{\mathrm{B}}$, and $-(d_{\mathrm{R}}-d_{\mathrm{B}})i_{\mathrm{G}}$ in Eq. 8, respectively. u and v represent a pixel of an input image. As described in Sec. 3.4, because Eq. 8 assumes that specular polarization is larger than diffuse polarization, the estimated illuminations are less reliable than the one from achromatic pixels. Therefore, we introduced a fixed parameter α to consider the difference in reliability. However, as mentioned in Sec. 5, estimated results from chromatic pixels are more accurate when scenes include blue skies. It is our future work to develop a more novel algorithm to determine α flexibly.

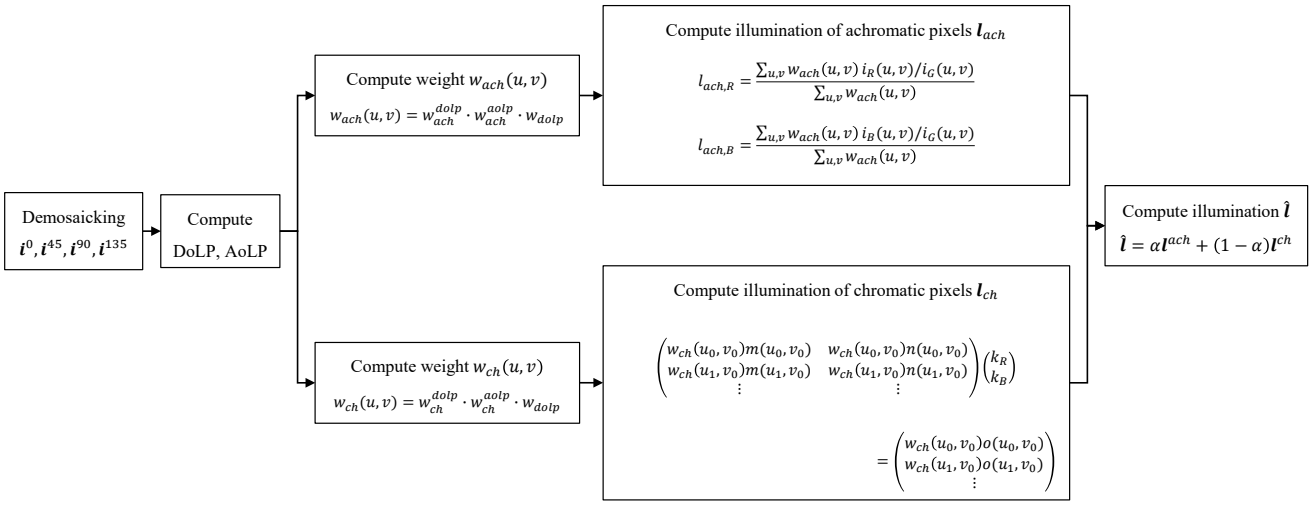

Figure 3. Flow chart describing the process from demosaicking to the final result $\hat{\boldsymbol{l}}$.

References

[1] Mahmoud Afifi, Jonathan Barron, Chloe LeGendre, Yun-Ta Tsai, and Francois Bleibel. Cross-camera convolutional color constancy. In *Int. Conf. Comput. Vis.*, pages 1981–1990, 2021. 3

[2] Gary Atkinson and Edwin Hancock. Multi-view surface reconstruction using polarization. *Int. Conf. Comput. Vis.*, 1:309–316, 2005. 1

[3] Jonathan Barron and Yun-Ta Tsai. Fast Fourier color constancy. In *Conf. Comput. Vis. Pattern Recog.*, pages 6950–6958, 2017. 3

[4] Gershon Buchsbaum. A spatial processor model for object colour perception. *J. Franklin Inst.*, 310(1):1–26, 1980. 3

[5] Dongliang Cheng, Dilip Prasad, and Michael Brown. Illuminant estimation for color constancy: Why spatial-domain methods work and the role of the color distribution. *J. Opt. Soc. Am. A*, 31(5):1049–1058, May 2014. 3

[6] Achuta Kadambi, Vage Taamazyan, Boxin Shi, and Ramesh Raskar. Polarized 3D: high-quality depth sensing with polarization cues. In *Int. Conf. Comput. Vis.*, pages 3370–3378, Dec 2015. 1

[7] Teppei Kurita, Shun Kaizu, Yuhi Kondo, Yasutaka Hirasawa, and Ying Lu. Image processing device and image processing method. U.S. Patent 10,460,422, issued Oct. 29, 2019. 2

[8] Edwin Land. The retinex theory of color vision. *Sci. Amer.*, 237(6):108–129, 1977. 3

[9] Matteo Rizzo. FC4-pytorch: A pytorch implementation of FC4: Fully convolutional color constancy with confidence-weighted pooling. https://github.com/matteo-rizzo/fc4-pytorch, Jul 2021. (Accessed on 22/11/2021). 3

[10] Matthias Sajjaa and Gregor Fischer. Automatic white balance: Whitebalpr using the dichromatic reflection model. In *Soc. Photo-Op. Inst. Eng. Conf. Series*, volume 7250, page 72500D, 2009. 3

[11] Joost van de Weijer, Theo Gevers, and Arjan Gijsenij. Edge-based color constancy. *Trans. Image Process.*, 16(9):2207–2214, 2007. 3

[12] Lawrence Wolff and Terrance Boult. Constraining object features using a polarization reflectance model. *Trans. Pattern Anal. Mach. Intell.*, 13(7):635–657, July 1991. 1

[13] Huanglin Yu, Ke Chen, Kaiqi Wang, Yanlin Qian, Zhaoxiang Zhang, and Kui Jia. Cascading convolutional color constancy. In *Conf. on Artif. Intell.*, pages 12725–12732, 2020. 2, 3